

## Durham Research Online

---

### Deposited in DRO:

04 October 2017

### Version of attached file:

Accepted Version

### Peer-review status of attached file:

Peer-reviewed

### Citation for published item:

Hattori, G. and Trevelyan, J. (2017) 'An overview of the peridynamics (PD) formulation with the extended boundary element method (XBEM) for dynamic fracture.', in 18th International Conference on Boundary Element Techniques : Bucharest, Romania, 11-13 July 2017 ; proceedings. , pp. 64-70.

### Further information on publisher's website:

<http://beteq.engineeringconferences.net/new/>

### Publisher's copyright statement:

### Additional information:

---

### Use policy

The full-text may be used and/or reproduced, and given to third parties in any format or medium, without prior permission or charge, for personal research or study, educational, or not-for-profit purposes provided that:

- a full bibliographic reference is made to the original source
- a [link](#) is made to the metadata record in DRO
- the full-text is not changed in any way

The full-text must not be sold in any format or medium without the formal permission of the copyright holders.

Please consult the [full DRO policy](#) for further details.

# An overview of the peridynamics (PD) formulation with the extended boundary element method (XBEM) for dynamic fracture

G. Hattori<sup>1\*</sup> and J. Trevelyan<sup>1</sup>

<sup>1</sup> School of Engineering & Computing Sciences, Durham University, DH1 3LE, Durham, UK.  
gabriel.hattori@durham.ac.uk, jon.trevelyan@durham.ac.uk

**Keywords:** Peridynamics, XBEM, dynamic fracture.

## Abstract.

Fracture mechanics problems have been addressed using the boundary element method (BEM) for many years, and more recently with the extended boundary element method (XBEM). However, fracture analysis of dynamic crack propagation with BEM have not considered dynamic effects such as crack branching (when a crack tip generates two others) or crack initiation. It is very complicated to capture the dynamic behaviour at the crack tip that can lead to crack branching. A recently developed numerical approach denominated peridynamics (PD) has shown great potential in modelling complex crack propagation behaviour, including crack branching. However, since it is a particle-based method, it requires a great amount of computational time, which can be impractical for large problems.

In this work we combine PD and XBEM for the study of dynamic fracture problems. A PD zone is defined around the crack tip, and it will receive the displacements from the XBEM solution. If the crack propagation criteria are satisfied, the bonds between the particles in the PD zone will break, generating a new crack path. This crack path is further discretised with the XBEM mesh. The advantage of this procedure is to reduce the computational costs of a modelling the problem using only PD particles. An example will be shown to illustrate the potential of the proposed approach.

## Introduction

The boundary element method (BEM) has been used in fracture mechanics problems for many years. The capability of providing high accuracy and stable results for the stress field around the crack tip is still not achievable by domain discretisation methods such as the finite element method (FEM). More recently, an extended boundary element method (XBEM) formulation has been implemented by the authors [1, 2] so the stress intensity factors (SIF) become part of the solution of the displacements field, therefore eliminating the post-processing step to calculate the SIF. However, BEM and XBEM have not been used to model dynamic effects properly.

Peridynamics (PD) is a novel formulation where continuum mechanics is discretised in terms of particles, which interact with each one through physical connections entitled bonds. The formulation was first proposed by Silling [3] and it has gained attention from the fracture community in recent years. The main advantage of this framework is that no special assumptions have to be made when dealing with discontinuities in the domain. This implies that PD can easily model complex crack propagation behaviour, such as crack initiation and crack branching, which is very difficult to model with boundary elements. However, PD is a particle-based method, which normally requires a high number of particles to model the problem adequately.

In this paper we present an overview on how to couple the XBEM and PD frameworks. Initially the XBEM analysis is performed, then the displacements are passed to a PD zone around the crack tip. The PD model then evaluates if the bonds will break, leading to crack propagation of even the initiation of cracks in other areas. This approach can use the advantage of both numerical methods and avoid the high computational cost associated to PD.

## Governing equations

The equation of motion in the presence of body forces  $\mathbf{b}$  is defined as

$$\sigma_{ij,j} + b_i = \rho \ddot{u}_i \quad (1)$$

where  $\rho$  is the mass density and  $\ddot{u}_i$  stands for the acceleration.

Symmetry applies for the stress and strain tensors, i.e.:

$$\sigma_{ij} = \sigma_{ji}; \quad \varepsilon_{ij} = \varepsilon_{ji} \quad (2)$$

where

$$\varepsilon_{ij} = \frac{1}{2}(u_{i,j} + u_{j,i}) \quad (3)$$

and  $u_i$  stands for the displacement on the  $i$ -direction.

The linear constitutive equations are given by the generalised Hooke's law

$$\sigma_{ij} = C_{ijkl}\varepsilon_{kl} \quad (4)$$

where  $C_{ijkl}$  define the material constants tensor, satisfying the following symmetry relations

$$C_{ijkl} = C_{jikl} = C_{ijlk} = C_{klij} \quad (5)$$

The deformation gradient  $\mathbf{F}(\mathbf{x})$  characterises the behaviour of motion in the neighbourhood of a material point  $\mathbf{x}$ , and it is defined as [4]

$$\mathbf{F}(\mathbf{x}) = \frac{\partial \mathbf{y}}{\partial \mathbf{x}} \quad (6)$$

where  $\mathbf{x}$  stands for the an arbitrary particle in the reference configuration, and  $\mathbf{y} = \mathbf{x} + \mathbf{u}$  stands for the particle in the deformed configuration. The deformation gradient is in principle not symmetric. The determinant of the deformation gradient is defined as  $J = \det(\mathbf{F}(\mathbf{x}))$ , and it is a measure of the volume increase. Since  $J > 0$ , the inverse of the deformation gradient can always be obtained.

The first Piola-Kirchhoff stress is given by

$$\mathbf{P}(\mathbf{x}) = J\boldsymbol{\sigma}\mathbf{F}(\mathbf{x})^T \quad (7)$$

## Peridynamics (PD)

The equation of motion in the PD framework is redefined as [3]

$$\rho\ddot{\mathbf{u}}(\mathbf{x}, t) = \int_{\mathcal{H}} \mathbf{f}(\mathbf{u}(\mathbf{x}', t) - \mathbf{u}(\mathbf{x}, t), \mathbf{x}' - \mathbf{x})dV_{x'} + \mathbf{b}(\mathbf{x}, t) \quad (8)$$

where  $\mathbf{f}$  is the pairwise force function that the particle  $\mathbf{x}'$  exerts on the particle  $\mathbf{x}$ ,  $\mathcal{H}$  is the neighbourhood of  $\mathbf{x}$ . This definition is also known as bond-based PD.

Figure 1 depicts the horizon of a particle  $\mathbf{x}$ . The horizon  $\delta$  can be considered as a cut-off influence area of any given particle. The interaction between particles is defined as a bond, which in continuum mechanics could also be considered as a spring connecting two particles. This definition is fundamentally the difference between the classical theory and PD, where the main idea is the direct contact between two particles.

## State-based peridynamics

The original PD formulation proposed in [3] has a critical limitation: it constrains the Poisson ratio to a fixed value. This issue arise from the fact that the bond-based formulation does not take into account that each one of the particles also possess its own horizon. This issue has been solved with a generalisation of the PD framework in [5], denominated state-based PD. In this case, the equation of motion is defined as

$$\int_{\mathcal{H}} \{\underline{\mathbf{T}}[\mathbf{x}, t]\langle \mathbf{x}' - \mathbf{x} \rangle - \underline{\mathbf{T}}[\mathbf{x}', t]\langle \mathbf{x} - \mathbf{x}' \rangle\}dV_{x'} + \mathbf{b}(\mathbf{x}, t) = \rho\ddot{\mathbf{u}}(\mathbf{x}, t) \quad (9)$$

with  $\underline{\mathbf{T}}$  as the force vector state field, and square brackets denote that the variables are taken in the state vector framework.

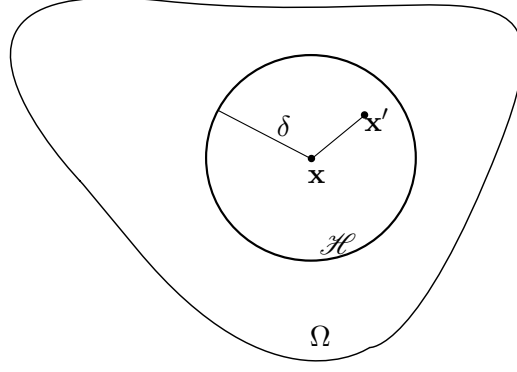


Figure 1: Horizon of a particle.

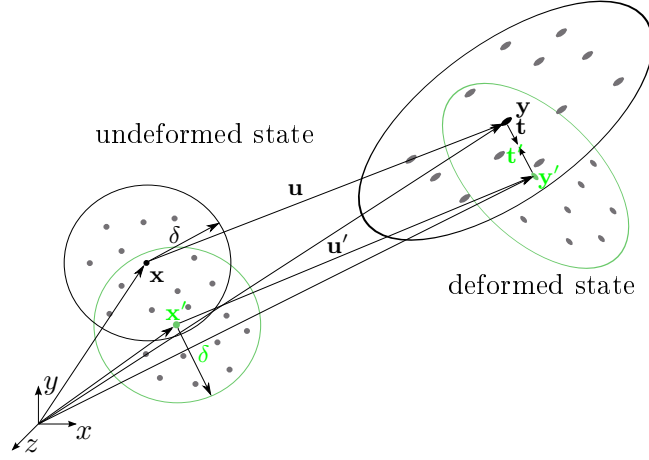


Figure 2: Reference and deformed configuration in state-based PD.

Figure 2 illustrates the reference (or initial) configuration, and the deformed configuration after a displacement  $\mathbf{u}$  and  $\mathbf{u}'$  has been imposed on particles  $\mathbf{x}$  and  $\mathbf{x}'$ , respectively.

There are 2 types of state-based formulation: ordinary and non-ordinary. In the ordinary theory, the forces in the bonds are defined in the direction of the bonds, in the same way as in the bond-based formulation. However, in ordinary state-based the forces in the bonds can have different magnitudes. In this case, the equilibrium is satisfied for every particle at the same time, in a similar as in other numerical methods. The main issue of the ordinary state-based theory is how to obtain the equivalent material properties from the classical continuum mechanics. An energy equivalent approach can be used, as detailed in Madenci and Oterkus [6].

In the non-ordinary theory, the forces in the bond are free to assume any direction, since parameters of continuum mechanics are employed, allowing for a generalisation. Another particularity of non-ordinary PD is that the constitutive matrix can be used directly in the formulation. In this paper we focus on the non-ordinary state-based formulation.

The PD state-based formulation consists in the use of state fields, which are explained in detail in Ref. [5]. For instance, the deformation vector state field is stated as

$$\underline{\mathbf{Y}}[\mathbf{x}, t](\xi) = \mathbf{y}(\mathbf{x} + \xi, t) - \mathbf{y}(\mathbf{x}, t) \quad (10)$$

The non-local deformation gradient  $\mathbf{F}(\mathbf{x})$  for each particle is given by

$$\mathbf{B}(\mathbf{x}) = \left[ \int_{\mathcal{H}} \omega(|\xi|)(\xi \otimes \xi) dV_{\xi} \right]^{-1} \quad (11)$$

$$\mathbf{F}(\mathbf{x}) = \left[ \int_{\mathcal{H}} \omega(|\xi|)(\underline{\mathbf{Y}}(\xi) \otimes \xi) dV_{\xi} \right] \cdot \mathbf{B}(\mathbf{x}) \quad (12)$$

where  $\mathbf{B}(\mathbf{x})$  is the shape tensor,  $\otimes$  denotes the dyadic product of two vectors, and  $\omega(|\xi|)$  is a dimensionless weight function, used to increase the influence of the nodes closes to  $\mathbf{x}$ . In this work, we assumed that  $\omega(|\xi|) = 1$ .

To incorporate the kinematic stress into the PD model, the transpose of the first Piola-Kirchhoff stress is equivalent to [7]

$$\mathbf{P}(\mathbf{x})^T = \frac{\partial W}{\partial \mathbf{F}} \quad (13)$$

with  $W$  being the strain energy density function.

The force vector at time  $t$  is finally stated as [7]

$$\underline{\mathbf{T}}[\mathbf{x}, t] \langle \mathbf{x}' - \mathbf{x} \rangle = \omega(|\mathbf{x}' - \mathbf{x}|) \mathbf{P}(\mathbf{x})^T \cdot \mathbf{B}(\mathbf{x}) \cdot (\mathbf{x}' - \mathbf{x}) \quad (14)$$

## Damage

In PD, damage is defined when a bond between two particles is broken. There are several damage criteria, but here we use one based on the critical deviatoric deformation [8]. We define the Lagrangian strain  $\mathbf{E}(\mathbf{x})$  as

$$\mathbf{E}(\mathbf{x}) = \frac{1}{2} (\mathbf{F}(\mathbf{x})^T \mathbf{F}(\mathbf{x}) - \mathbf{I}) \quad (15)$$

Next we calculate the equivalent strain

$$E_{eq}(\mathbf{x}, \mathbf{x}') = \sqrt{\frac{4}{3} I_2'} = \sqrt{\frac{2}{3} E_{ij}'(\mathbf{x}, \mathbf{x}') E_{ij}'(\mathbf{x}, \mathbf{x}')} \quad (16)$$

where

$$E_{ij}'(\mathbf{x}, \mathbf{x}') = E_{ij}(\mathbf{x}, \mathbf{x}') - \frac{1}{3} E_{kk}(\mathbf{x}, \mathbf{x}') \quad (17)$$

$$E_{ij}(\mathbf{x}, \mathbf{x}') = \frac{1}{2} (\mathbf{E}(\mathbf{x}) + \mathbf{E}(\mathbf{x}')) \quad (18)$$

If  $E_{eq}(\mathbf{x}, \mathbf{x}') \geq E_{crit}$ , then the bond between  $\mathbf{x}$  and  $\mathbf{x}'$  will break. We define the function  $\mu(\mathbf{x}, \mathbf{x}')$  as

$$\mu(\mathbf{x}, \mathbf{x}') = \begin{cases} 1 & \text{if } E_{eq}(\mathbf{x}, \mathbf{x}') < E_{crit} \\ 0 & \text{otherwise} \end{cases} \quad (19)$$

The damage index  $\varphi$  is obtained using the expression

$$\varphi = 1 - \frac{\int_{\mathcal{H}} \mu(\mathbf{x}, \mathbf{x}') dV_{x'}}{\int_{\mathcal{H}} dV_{x'}} \quad (20)$$

## Extended Boundary Element Method (XBEM)

The extended boundary element method (XBEM) has been developed by [1, 2] for isotropic and anisotropic materials, respectively. The method uses the information of the SIF to describe the displacements at the crack surfaces. In this way, the additional number of degrees of freedom of the problem is independent to the number of enriched elements, as is the case of other enrichment approaches such as in the extended finite element method (XFEM). Moreover, the SIF become part of the unknowns of the problem, so there is no need for evaluating the J-integral or the interaction integral to obtain the SIF.

The XBEM formulation uses a dual approach, where the fracture problem is discretised using a displacement boundary integral equation (DBIE) and a traction boundary integral equation (TBIE). The DBIE and TBIE for the XBEM are defined as

$$c_{ij}(\boldsymbol{\xi}) u_j(\boldsymbol{\xi}) + \int_{\Gamma} p_{ij}^*(\mathbf{x}, \boldsymbol{\xi}) u_j(\mathbf{x}) d\Gamma(\mathbf{x}) + \int_{\Gamma_c} p_{ij}^*(\mathbf{x}, \boldsymbol{\xi}) \tilde{K}_l \psi_{lj}(\boldsymbol{\xi}) d\Gamma = \int_{\Gamma} u_{ij}^*(\mathbf{x}, \boldsymbol{\xi}) p_j(\mathbf{x}) d\Gamma(\mathbf{x}) \quad (21)$$

$$c_{ij}(\boldsymbol{\xi}) p_j(\boldsymbol{\xi}) + N_k \int_{\Gamma} s_{kij}^*(\mathbf{x}, \boldsymbol{\xi}) u_j(\mathbf{x}) d\Gamma(\mathbf{x}) + N_k \int_{\Gamma_c} s_{kij}^*(\mathbf{x}, \boldsymbol{\xi}) \tilde{K}_l \psi_{lj}(\boldsymbol{\xi}) d\Gamma = N_k \int_{\Gamma} d_{kij}^*(\mathbf{x}, \boldsymbol{\xi}) p_j(\mathbf{x}) d\Gamma(\mathbf{x}) \quad (22)$$

where  $\Gamma$  represents the boundaries,  $\Gamma_c = \Gamma_+ \cup \Gamma_-$  stands for the crack surfaces  $\Gamma_+$  and  $\Gamma_-$ ,  $N_k$  is the normal at the observation point,  $\tilde{K}_l$  are the additional degrees of freedom ( $K_I$  and  $K_{II}$  in this case) and  $\psi_{lj}$  are the enrichment function which describe the asymptotic behaviour of the displacement field around the crack tip;  $u_{ij}^*$  and  $p_{ij}^*$  are the displacement and traction fundamental solutions, while  $d_{kij}^*$  and  $s_{kij}^*$  are obtained through derivation and further application of the generalised Hooke's law on the  $u_{ij}^*$  and  $p_{ij}^*$  kernels, respectively. Let us remark that strongly singular and hypersingular terms arise from the integration of the  $p_{ij}^*$ ,  $d_{rij}^*$  and  $s_{rij}^*$  kernels and they are need to be regularised before any numerical integration scheme can be used. The regularisation procedures for both the DBIE and the TBIE are detailed in [2].

### Combined framework of XBEM and PD

The fracture problem is initially solved with the XBEM to obtain the displacement field and the SIF. Next, we select a small zone around the crack tip, and enforce that the displacement calculated with XBEM will be the input for the PD, i.e.,  $u^{XBEM} = u^{PD}$ . The displacements can be obtained in two different ways: 1) using Eq. (21) (where  $c_{ij}(\xi) = 1$  for internal points); 2) since  $K_I$  and  $K_{II}$  are known, the expression of the asymptotic field around the crack tip can be used, which provides a good approximation in a faster way than calculating internal points (refer to [1, 2] for the expressions of the asymptotic displacements for isotropic and anisotropic materials, respectively).

The displacements are scaled over time to ensure that there is no abrupt variation of the displacement field in the PD domain. This issue could result in a high number of bonds being broken at the same time, hence leading to an higher damage estimation.

### Plate with an centred crack

We consider a square plate ( $w/h = 0.04$  m) with a centred crack of length  $2a = 0.02$ . The PD zone is defined to be a square zone of  $0.02a$  around the crack tip. Figure 3 illustrates how the PD zone is defined around the crack tip. The material is aluminium, with  $E = 69$  GPa and  $\nu = 0.33$ . The XBEM model is subject to a uniform static load of  $\sigma = 1$  MPa.

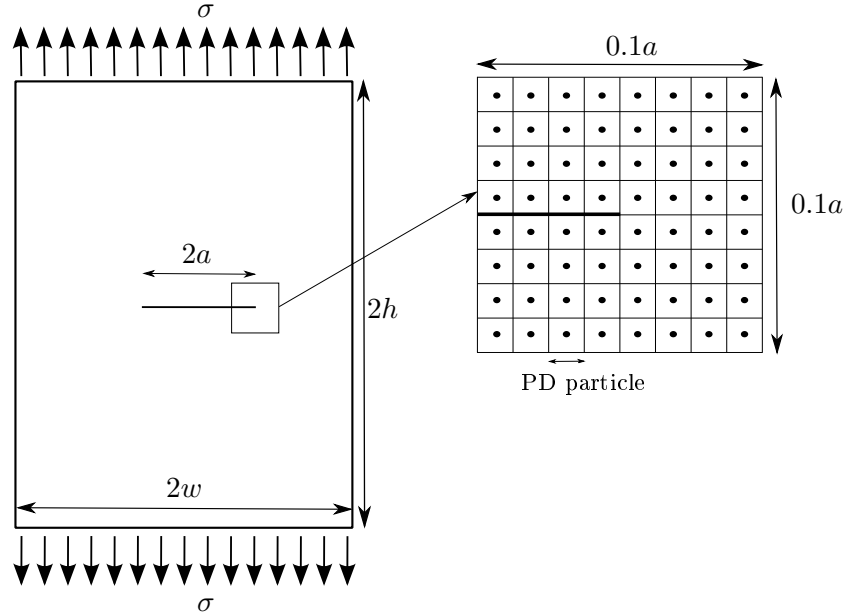


Figure 3: Coupling between XBEM and PD.

We assumed that there are some inclusions that are not considered by the XBEM model, but can have an effect on the crack propagation in the PD model. The material properties of the inclusions are:  $E_{inc} = 10E$ ,  $\nu = 0.33$ . To evaluate properly how PD can perform, we also included a velocity load at the crack surfaces.

Figure 4 illustrates the damage index  $\varphi$  of the PD model with inclusions and Figure 5 depicts the same for the case without inclusions. One can observe that there are small damaged areas that appear

on the top and bottom of the crack surfaces. Since there are some inclusions close to these areas, they act as reflecting boundaries, so that the displacements in that zone will be higher, further leading to some of the bonds breaking. This kind of damage initiation is complicated to model with XBEM and XFEM, since it requires more assumptions than the linear elastic fracture mechanics theory.

From Figure 5, no damage appears on the top and bottom of the crack surfaces, and the crack propagates perpendicularly to the direction of the maximum stress. The same crack growth rate can be verified from both the inclusion and no inclusion examples. However, inclusions can have a stress shielding effect, for example, if there would be an inclusion close to the crack tip, the crack would not have sufficient energy to grow.

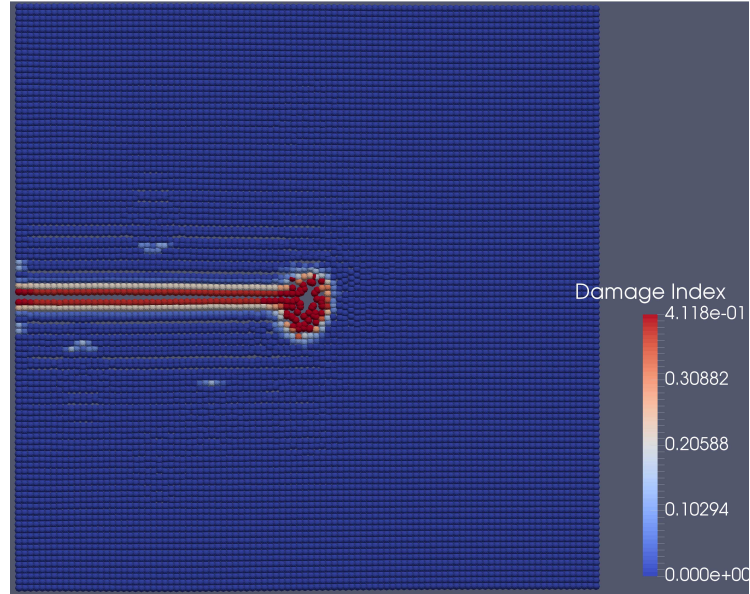


Figure 4: PD zone - with inclusions.

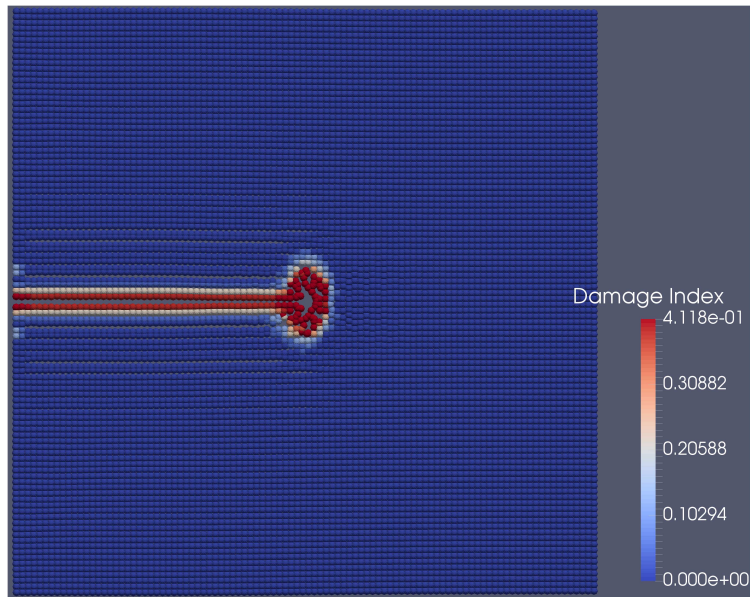


Figure 5: PD zone - no inclusions.

## Conclusions

We presented an example on how to use both XBEM and PD for evaluating some dynamic effects. Some damage has been detected coming from reflection of the waves induced by a velocity field at the crack surfaces. The results presented in this work are still preliminary. A more detailed coupling between XBEM and PD is necessary in order to explore the advantages of this new framework, which is work in progress from the authors.

## Acknowledgements

The first author acknowledges the Faculty of Science, Durham University, for his Postdoctoral Research Associate funding.

## References

- [1] I. A. Alatawi and J. Trevelyan. A direct evaluation of stress intensity factors using the extended dual boundary element method. *Engineering Analysis with Boundary Elements*, 52:56–63, 2015.
- [2] G. Hattori, I. A. Alatawi, and J. Trevelyan. An extended boundary element method formulation for the direct calculation of the stress intensity factors in fully anisotropic materials. *International Journal for Numerical Methods in Engineering*, 2016.
- [3] S. A. Silling. Reformulation of elasticity theory for discontinuities and long-range forces. *Journal of the Mechanics and Physics of Solids*, 48(1):175–209, 2000.
- [4] G. A. Holzapfel. *Nonlinear solid mechanics*. John Wiley & Sons Ltd, 2000.
- [5] S. A. Silling, M. Epton, O. Weckner, J. Xu, and E. Askari. Peridynamic states and constitutive modeling. *Journal of Elasticity*, 88(2):151–184, 2007.
- [6] E. Madenci and E. Oterkus. *Peridynamic theory and its applications*. Springer, 2014.
- [7] S. A. Silling and R. B. Lehoucq. Convergence of peridynamics to classical elasticity theory. *Journal of Elasticity*, 93(1):13–37, 2008.
- [8] T. L. Warren, S. A. Silling, A. Askari, O. Weckner, M. A. Epton, and J. Xu. A non-ordinary state-based peridynamic method to model solid material deformation and fracture. *International Journal of Solids and Structures*, 46(5):1186–1195, 2009.